



Vaginal bacteria-derived extracellular vesicles diffuse through human cervicovaginal mucus to enable microbe-host signaling



Darby Steinman¹, Alyssa P. Petersen², Yasmi Chibber², Caleb Crawford², Pranshu Tyagi² & Hannah C. Zierden^{1,2,3,4} ✉

The composition of the vaginal microenvironment has significant implications for gynecologic and obstetric outcomes. Where a *Lactobacillus*-dominated microenvironment is considered optimal, a polymicrobial environment is associated with increased risk for female reproductive diseases. Recent work examined bacteria-derived extracellular vesicles (bEVs) as an important mode of microbe-host communication that may influence reproductive outcomes. However, in order to communicate with female reproductive tissues, bEVs must penetrate the protective cervicovaginal mucus barrier. We demonstrate increased diffusion of bEVs compared to whole bacteria. Additionally, we evaluate the uptake of bEVs by, and the resulting effects on, human vaginal epithelial, endometrial, and placental cells, highlighting potential mechanisms of action by which vaginal dysbiosis contributes to gynecologic and obstetric diseases. Taken together, our work demonstrates the ability of bEVs to mediate female reproductive outcomes and highlights their potential as therapeutic modalities for treating dysbiosis and dysbiosis-associated diseases in the female reproductive tract.

The composition of the vaginal microbiome significantly influences gynecologic and obstetric outcomes. Unlike most microbial communities in the human body, an optimal vaginal microbiome is one dominated by lactobacilli, which produce antimicrobial, antiviral, and antifungal agents that protect the local environment^{1–5}. However, 30% of women in the U.S. are affected by vaginal dysbiosis, which is characterized as a polymicrobial environment colonized by pathogenic species including *Gardnerella vaginalis* and *Mobiluncus mulieris*^{6,7}. Vaginal dysbiosis contributes to an increased risk for sexually transmitted infections, pelvic inflammatory disease, and preterm birth, as well as adverse neonatal outcomes^{8–13}.

Dysbiosis-associated microbes produce enzymes that degrade the cervicovaginal mucus barrier, reduce epithelial barrier integrity, and cause inflammation in local tissues^{12,14,15}. Hypotheses surrounding microbial communication to upper levels of the female reproductive tract suggest that vaginal microbes can ascend into the uterine environment, causing infection and inflammation which contributes to adverse women's health outcomes¹⁶. Ascension to upper levels of the female reproductive tract would require bacteria to diffuse through the protective cervicovaginal mucus (CVM)

barrier. CVM is a complex mixture of glycoproteins, ions, lipids, cells, and bacteria that protects the female reproductive tract from infections^{17–19}. Mucin proteins are crosslinked to form a heterogeneous pore structure that sterically hinders the mobility of large pathogens, while the electrostatic and hydrophobic regions on these proteins adhesively trap charged virions and particles¹⁷. In the context of dysbiosis, sialidases produced by *G. vaginalis* weaken mucus barrier properties and permit the diffusion of larger particles^{20,21}. Indeed, we previously quantified the pore size of mucus samples characterized by a dysbiotic microbiome and reported a significantly larger pore size than mucus samples dominated by *L. crispatus* (considered healthy)²². However, even the larger pore size of mucus samples associated with a dysbiotic microbiome was found to be too small for microbes to efficiently penetrate and reach the uterus²². Given these findings, we hypothesized that whole microbes would be too large to move freely through the mucus structure, preventing direct communication between bacterial cells and host cells. Thus, we sought to explore modes of microbial signaling that may directly alter tissue function in upper levels of the female reproductive tract. Specifically, we hypothesized that vaginal microbe-derived

¹Fischell Department of Bioengineering, University of Maryland, College Park, MD, USA. ²Department of Chemical & Biomolecular Engineering, University of Maryland, College Park, MD, USA. ³Robert E. Fischell Institute for Biomedical Devices, College Park, MD, USA. ⁴Department of Obstetrics, Gynecology and Reproductive Sciences, University of Maryland School of Medicine, Baltimore, MD, USA. ✉e-mail: hzierden@umd.edu

extracellular vesicles play a critical role in microbe-host communication to female reproductive tract tissues.

Bacteria-derived extracellular vesicles (bEVs) are microbe-derived, nano-sized, membrane-bound particles that enable microbe-host and microbe-microbe communication throughout the body^{23,24}. bEVs are spontaneously produced by both Gram-positive and Gram-negative bacteria, and facilitate horizontal gene transfer, defense against the host immune system, and transport of virulence factors^{23,25}. Emerging work describes the role of bEVs in mediating tissue function and disease outcomes in the lower female reproductive tract^{26–29}. These reports lay a foundation for understanding the role of bEVs in mediating gynecologic and obstetric outcomes. However, further work is necessary to understand the fate of bEVs in biological barriers (namely, CVM), and how bEVs regulate tissue function in the female reproductive tract.

Here, we sought to test the hypothesis that bEVs are capable of mediating microbial communication to upper levels of the female reproductive. As such, we: (1) evaluated the mobility of both whole bacteria and bEVs through CVM to assess the potential for ascension into the uterine environment; (2) assessed bEV uptake by female reproductive tract cell types; and (3) established the role of bEVs in altering tissue function relevant to the female reproductive tract. To our knowledge, this work is the first to quantify the mobility of bEVs in human CVM, with direct comparisons to whole bacteria. We report changes to vaginal epithelial, endometrial, and placental cells mediated by bEVs derived from both healthy-associated and

dysbiotic-associated species of human vaginal bacteria (*L. crispatus*, *L. iners*, *G. vaginalis*, and *M. mulieris*). Taken together, our work points towards potential mechanisms by which vaginal bacteria-derived bEVs contribute to female reproductive tract disease and lays a foundation for future work to develop next generation therapies for preventing and treating adverse gynecologic and obstetric outcomes.

Results

Physical characteristics of bacteria-derived extracellular vesicles differ based on cell of origin

Throughout this work, we evaluated differences in bEVs isolated from human-derived, commercially available strains of *L. crispatus*, *L. iners*, *G. vaginalis*, and *M. mulieris*. *L. crispatus* was used as a representative of a healthy vaginal microbiome; *L. iners* representative of an intermediate microbiome; *G. vaginalis* representative of dysbiosis; and *M. mulieris* representative of advanced dysbiosis.

We first sought to examine the physical characteristics of bEVs derived from these four strains. bEVs were confirmed to be membrane-bound particles via TEM (Fig. 1A, Supplementary Fig. 1). bEV concentration was highest from *M. mulieris* cultures, followed by *L. crispatus* > *L. iners* > *G. vaginalis*. *G. vaginalis*-derived bEVs were significantly lower in concentration ($1.18 \pm 0.21 \times 10^9$) compared to bEVs isolated from *L. crispatus* ($2.05 \pm 0.16 \times 10^9$ particles/mL, $p = 0.0253$) and *M. mulieris* cultures ($2.14 \pm 0.24 \times 10^9$ particles/mL, $p = 0.0196$, Fig. 1B, C). Normalized to colony

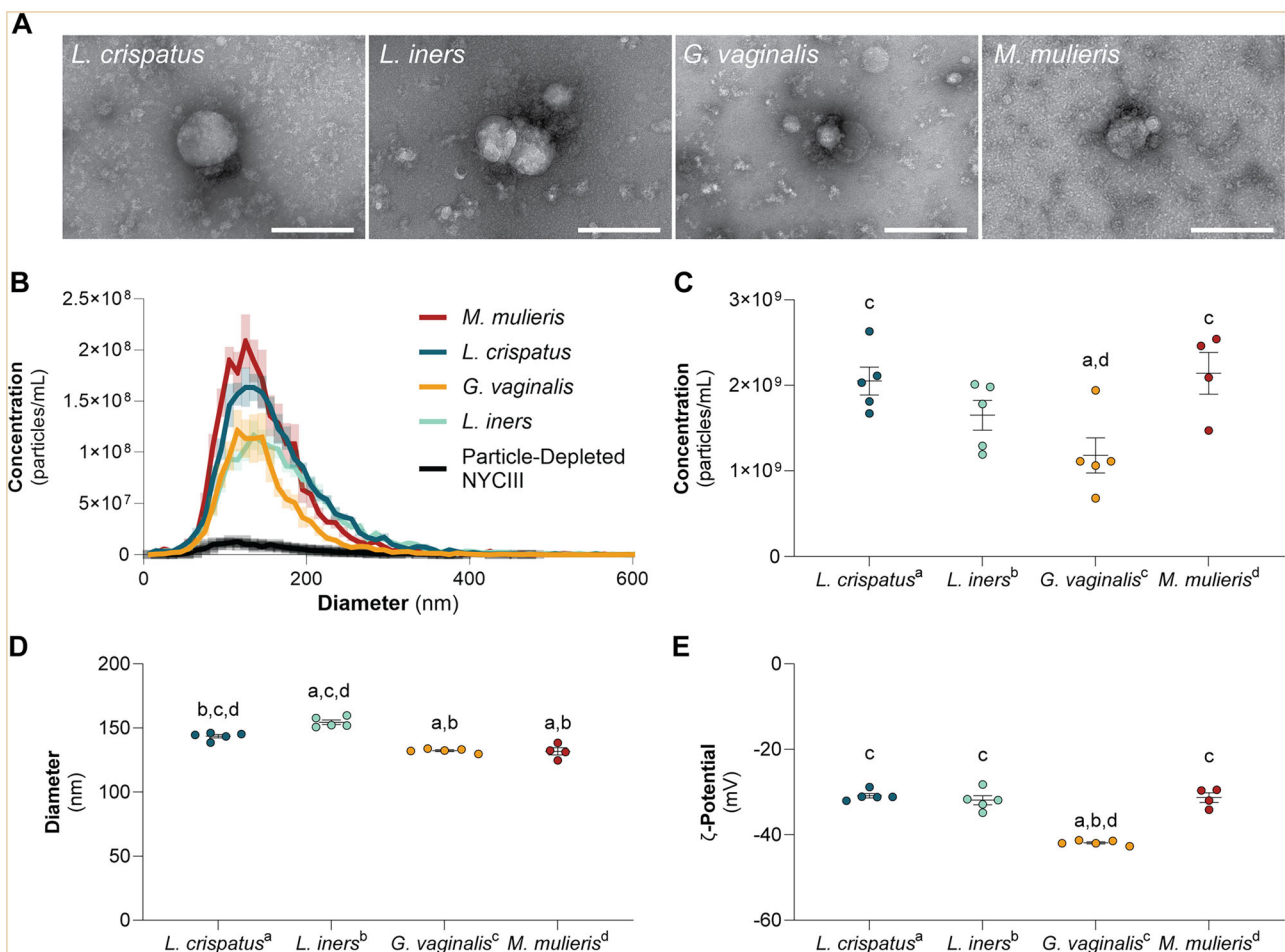
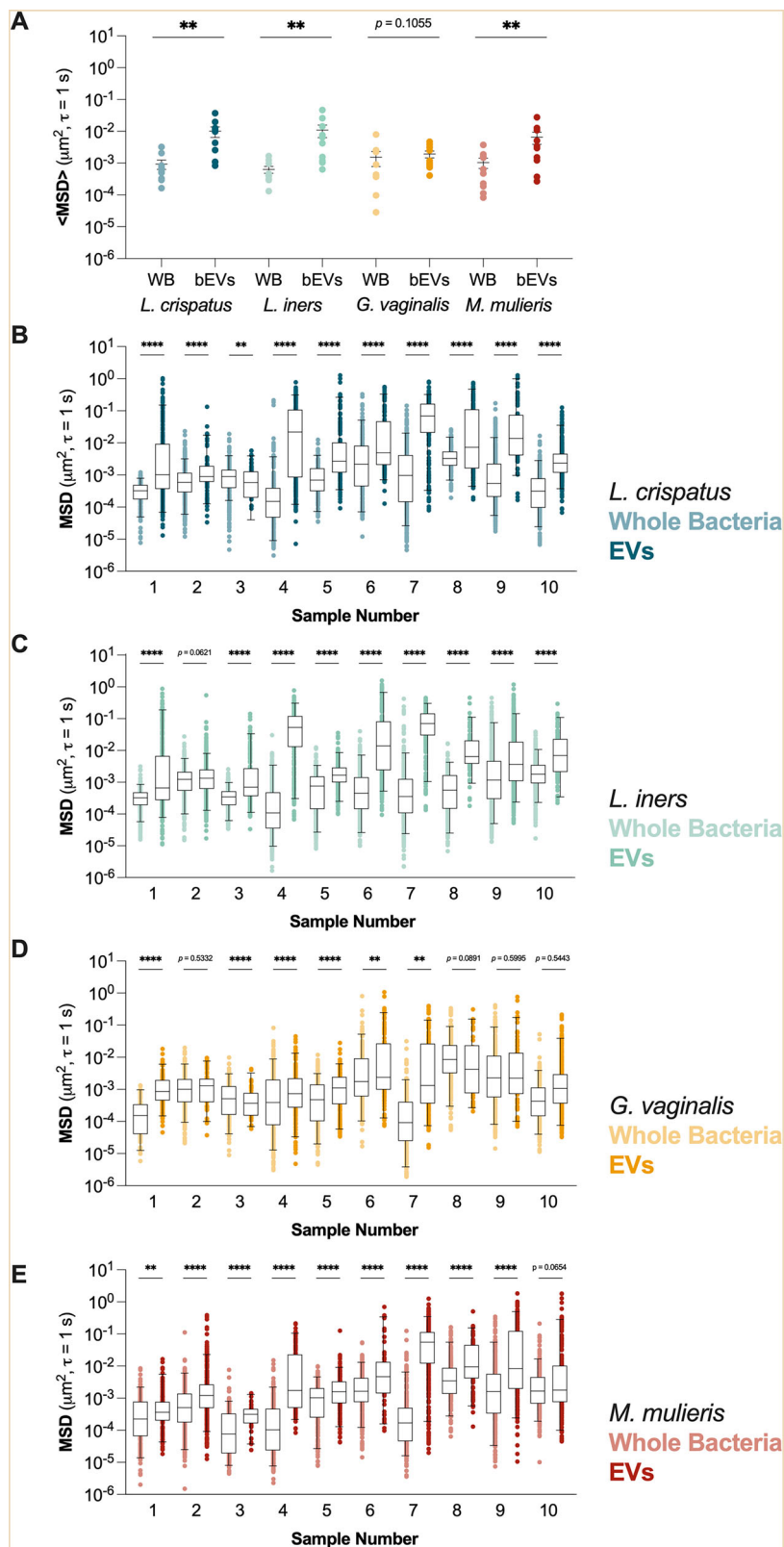


Fig. 1 | Physical characteristics of vaginal bacteria-derived bEVs. A Isolated bEVs were membrane-bound particles, as imaged via TEM. Scale bars denote 200 nm. **B, C** *M. mulieris* cultures produced the most bEVs, followed by *L. crispatus* > *L. iners* > *G. vaginalis*. **D** *L. iners*-derived bEVs were largest in diameter, followed by *L. crispatus* > *G. vaginalis* > *M. mulieris*-derived bEVs. **E** The ζ-potential of *G. vaginalis*-derived bEVs was the most negative, followed by *L. iners* < *M. mulieris* < *L. crispatus*-

derived bEVs. Data are shown as mean ± SEM. Statistical significance ($p \leq 0.05$) was calculated by one-way ANOVA with Tukey post hoc multiple comparison tests and is represented by a letter corresponding to the species of comparison (a, *L. crispatus*; b, *L. iners*; c, *G. vaginalis*; d, *M. mulieris*). Outliers removed in accordance with Grubb's outlier test.

Fig. 2 | Whole bacteria show limited mobility across all species. **A** Geometric means of the mean squared displacement at one second for whole bacteria and bEVs in $n = 10$ samples; $n = 5$ high pH (> 4.2), $n = 5$ low pH (≤ 4.2). bEVs exhibited increased mobility compared to whole bacteria. Significance was determined using Wilcoxon matched-pairs signed rank tests for each bEV-whole bacterial pair. **B** Across all CVM samples, *L. crispatus* whole bacteria exhibited limited diffusion compared to bEVs. **C** In 9/10 samples, *L. iners* whole bacteria exhibited limited diffusion compared to bEVs. **D** In 6/10 samples, *G. vaginalis* whole bacteria exhibited limited diffusion compared to bEVs. **E** In 9/10 samples, *M. mulieris* whole bacteria exhibited limited diffusion compared to bEVs. Box and Whiskers are shown as 5-95% confidence intervals. Samples are ordered from low to high pH. Two-tailed Mann-Whitney non-parametric tests were performed to compare whole bacteria and bEV mobility in each individual participant. ($n = 10$ CVM samples, $*p \leq 0.05$, $**p \leq 0.01$, $***p \leq 0.001$, and $****p \leq 0.0001$).



forming units, *L. crispatus* produced the most bEVs, followed by *L. iners* > *M. mulieris* > *G. vaginalis* (Supplementary Fig. 2A). *L. iners*-derived bEVs were the largest in diameter (154.5 ± 1.79 nm), compared to all other species ($p \leq 0.0015$, Fig. 1D). Additionally, *G. vaginalis*-derived bEVs (132.3 ± 0.71 nm) and *M. mulieris*-derived bEVs (131.7 ± 2.81 nm) were smaller than *L. crispatus*-derived bEVs (143.6 ± 1.33 nm, $p \leq 0.0011$). *G.*

vaginalis-derived bEVs had a lower ζ -potential (-41.87 ± 0.24 mV) compared to *L. crispatus*-derived bEVs (-30.85 ± 0.54 mV, $p < 0.0001$), *L. iners*-derived bEVs (-31.90 ± 1.07 mV, $p < 0.0001$), and *M. mulieris*-derived bEVs (-31.30 ± 1.11 mV, $p < 0.0001$, Fig. 1E). No differences in bEV protein content were observed (Supplementary Fig. 2B). The observed differences in size, surface charge (ζ -potential), and production may influence

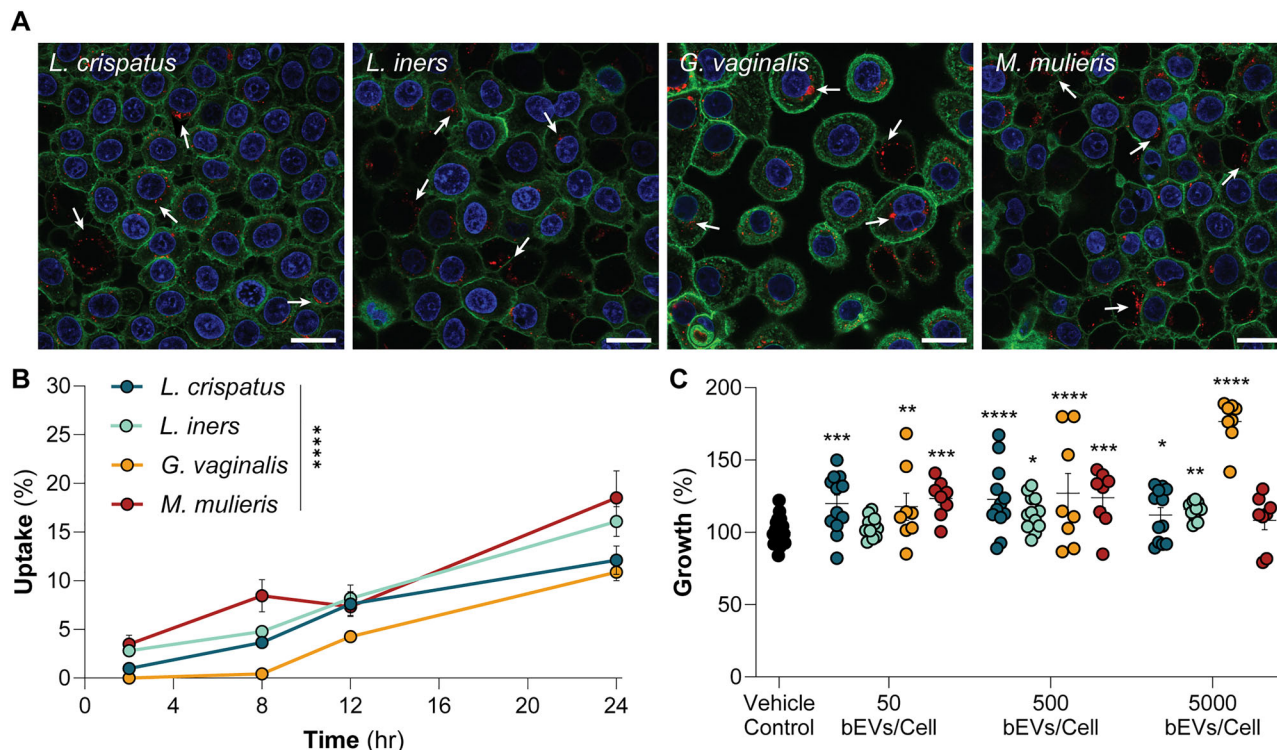


Fig. 3 | Vaginal epithelial cells internalize bEVs. A Confocal images revealed uptake of bEVs. Scale bars denote 20 μm . **B** Based on two-way ANOVAs, uptake assays determined that there were significant differences in the uptake based on bEV type. $n = 8\text{--}12$ per dose per timepoint. Replicates below the standard curve were assumed to be 0%. Vaginal epithelial cells internalized *M. mulieris*-derived bEVs significantly more than *L. crispatus*-derived bEVs or *G. vaginalis*-derived bEVs at

24 h. **C** Vaginal epithelial cell growth increased over 24 h in response to bEV treatment. Statistics were performed using two-way ANOVA. For viability experiments, Tukey post hoc multiple comparison tests were used to compare treatment groups to vehicle control. Outliers were removed in accordance with Grubb's outlier test. Data are shown as mean \pm SEM. * $p \leq 0.05$, ** $p \leq 0.01$, *** $p \leq 0.001$, and **** $p \leq 0.0001$.

bEV interactions with the vaginal microenvironment and female reproductive tract.

bEVs exhibit increased mobility in human cervicovaginal mucus compared to whole bacteria

To test the hypothesis that bEVs penetrate human CVM more efficiently than whole bacteria, we used multiple-particle tracking technology to determine individual particle mobility through CVM. To ensure comprehensive sampling, an equal number of participants samples with high and low pH CVM were utilized (pH above or below 4.2, $n = 5$ per group, Supp. Table 1). Across all samples, we observed increased mobility by bEVs, as compared to whole bacteria. Geometric means of the mean squared displacement (MSD) were determined using the 1 s time point (Fig. 2A). For *L. crispatus* whole bacteria and bEVs, all CVM samples exhibited limited mobility of whole bacteria compared to bEVs ($p \leq 0.0076$, Fig. 2B). For *L. iners*, 9/10 samples exhibited limited mobility of whole bacteria compared to bEVs (Fig. 2C, $p \leq 0.0001$). For *G. vaginalis*, 6 out of 10 samples exhibited limited mobility of whole bacteria compared to bEVs (Fig. 2D, $p \leq 0.01$). For *M. mulieris*, 9 out of 10 samples exhibited limited mobility of whole bacteria compared to bEVs ($p \leq 0.0001$, Fig. 2E). Previous work demonstrated that pH, as an indicator of dysbiosis, is positively correlated with particle mobility^{20,22}. Here, we investigated the mobility of both whole bacteria and bEVs in relation to sample pH (Supplementary Fig. 3). While we did not observe differences in whole bacteria or bEV mobility as a result of sample pH, this may be attributed to the relatively low sample size included in this study ($n = 5$ high pH (> 4.2), $n = 5$ low pH (≤ 4.2)). Regardless, our data suggests that bEVs are more diffusive than whole bacteria in CVM, even in the context of weakened barrier properties. Given the increased mobility of bEVs in CVM, compared to whole bacteria, we hypothesize that bEVs represent an important mediator of microbe-host communication in the female reproductive tract. We next sought to evaluate the interactions of

bEVs with female reproductive tract tissues, moving from vaginal epithelial cells to endometrial cells, and, finally, to the placenta.

Vaginal epithelial cells internalize bEVs in vitro

Based on the evidence that bEVs diffuse through CVM, we sought to determine the effect of bEVs on vaginal epithelial cells in vitro. After 24 h incubation, confocal microscopy verified bEV presence within cytosol (Fig. 3A, Supplementary Fig. 4). Uptake assays revealed significant differences in the uptake based on bEV parent cell (Fig. 3B). Specifically, vaginal epithelial cells internalized *M. mulieris*-derived bEVs ($18.52 \pm 2.78\%$) significantly more than *L. crispatus*-derived bEVs ($12.12 \pm 1.47\%$, $p = 0.0015$) or *G. vaginalis*-derived bEVs ($10.89 \pm 0.87\%$, $p = 0.0006$) at 24 h. *L. iners*-derived bEVs ($16.08 \pm 1.52\%$) demonstrated higher internalization compared to *G. vaginalis*-derived bEVs ($p = 0.0373$). Administration of bEVs was not detrimental to cellular growth (Fig. 3C). Rather, cell growth increased over 24 h, with the largest increase in growth observed in vaginal epithelial cells treated with *G. vaginalis*-derived bEVs at a dose of 5000 bEVs/cell ($176.5 \pm 5.52\%$, $p < 0.0001$). This may be attributed to protein and metabolite cargoes of the bEVs.

Endometrial cells internalize bEVs in vitro

Moving from the vaginal environment into the uterine environment, bEVs will encounter endometrial tissue. Thus, we investigated the endometrial cell response to vaginal bacteria-derived bEVs. Microscopy verified bEV internalization at 24 h (Fig. 4A, Supplementary Fig. 5). Again, uptake assays revealed significant differences in the uptake based on bEV parent cell (Fig. 4B). At 24 h, *M. mulieris*-derived bEVs ($7.99 \pm 0.84\%$) exhibited significantly lower internalization compared to *L. crispatus*-derived bEVs ($25.20 \pm 5.27\%$, $p < 0.0001$), *L. iners* bEVs ($20.73 \pm 4.97\%$, $p < 0.0001$), and *G. vaginalis*-derived bEVs ($19.16 \pm 0.67\%$, $p = 0.0045$). Consistent with our observations in vaginal epithelial cell cultures, administration of bEVs was

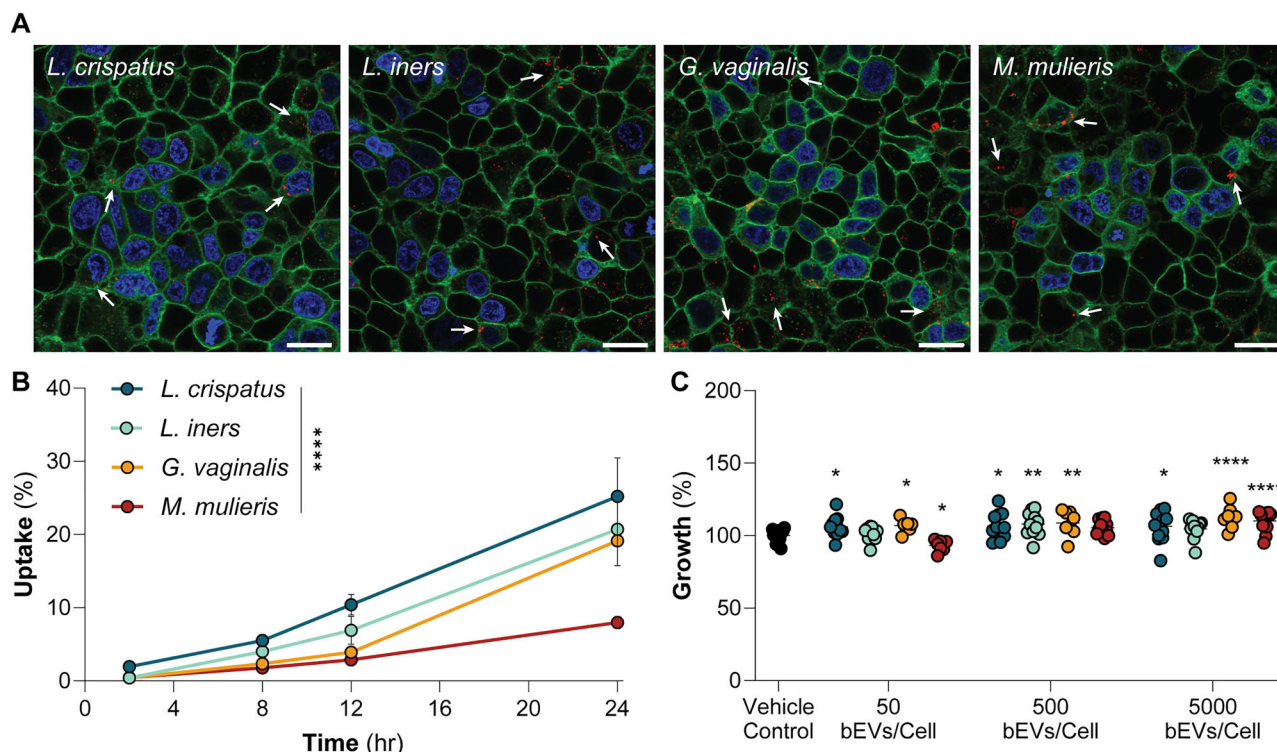


Fig. 4 | Endometrial cells internalize bEVs. **A** Confocal images revealed internalization of bEVs by endometrial cells. Scale bars denote 20 μ m. **B** *L. crispatus*-derived bEVs were most internalized, followed by *L. iners* -> *G. vaginalis* -> *M. mulieris*-derived bEVs. n = 8–12. **C** Endometrial cell growth increased over 24 h in response to bEV treatment. n = 8–12. Statistics were performed using two-way

ANOVA. For viability experiments, Tukey post hoc multiple comparison tests were used to compare treatment groups to vehicle control. Outliers were removed in accordance with Grubb's outlier test. Data are shown as mean \pm SEM. (* $p \leq 0.05$, ** $p \leq 0.01$, *** $p \leq 0.001$, and **** $p \leq 0.0001$).

not detrimental to cellular growth (Fig. 4C). Cell growth increased over 24 h, with the largest increase observed in cultures treated with *G. vaginalis*-derived bEVs at a dose of 5000 bEVs/cell ($112.2 \pm 2.62\%$, $p = 0.0007$).

Placental cells internalize bEVs in vitro

Given the critical role of the vaginal microbiome in pregnancy and neonatal outcomes, we next investigated bEV interactions with the placenta. Uptake experiments verified bEV presence within cells at 24 h (Fig. 5A, Supplementary Fig. 6), and uptake assays determined significant differences in the uptake based on bEV type (Fig. 5B). *L. crispatus*-derived bEVs were most internalized after 24 h compared to all other species ($39.71 \pm 1.99\%$, $p < 0.0001$). *L. iners*-derived bEVs ($20.39 \pm 3.13\%$) had greater uptake than both *G. vaginalis*-derived bEVs and *M. mulieris*-derived bEVs ($p < 0.0001$). *G. vaginalis*-derived bEVs ($11.21 \pm 0.91\%$) were more internalized than *M. mulieris*-derived bEVs ($5.58 \pm 0.68\%$, $p = 0.0052$). Consistent with vaginal epithelial and endometrial cells, we observed an increase in placental cell growth after treatment with *G. vaginalis*-derived bEVs at a dose of 5000 bEVs/cell ($118.9 \pm 7.38\%$, $p < 0.0001$, Fig. 5C).

bEV administration modulates cytokine response in female reproductive tract cells in vitro

Given our observed species-dependent bEV uptake and growth response, we sought to evaluate the change in cell function by measuring cytokine and chemokine production after bEV exposure. In vaginal epithelial cells, IL-6 production was increased in response to administration of *L. crispatus*- (2.24 ± 0.35 pg/mL, $p = 0.0013$), *G. vaginalis*- (4.06 ± 0.10 pg/mL, $p < 0.0001$), and *M. mulieris*-derived bEVs (3.35 ± 0.36 pg/mL, $p < 0.0001$) compared to vehicle controls (0.81 ± 0.12 pg/mL, Fig. 6A). Similarly, IL-8 production increased in response to *L. crispatus*- (44.94 ± 8.52 pg/mL, $p = 0.0003$), *G. vaginalis*- (86.78 ± 3.38 pg/mL, $p < 0.0001$), and *M. mulieris*-derived bEVs (102.3 ± 8.497 pg/mL, $p < 0.0001$) compared to vehicles

controls (8.98 ± 1.14 pg/mL, Fig. 6B). *M. mulieris*-derived bEVs (0.03 ± 0.004 pg/mL, $p = 0.0107$) resulted in an increase in IL-10 concentrations compared to controls (0.02 ± 0.004 pg/mL, Fig. 6C). IL-1 β concentrations increased after exposure to both *G. vaginalis*- (0.50 ± 0.01 pg/mL, $p < 0.0001$) and *M. mulieris*-derived bEVs (0.41 ± 0.04 pg/mL, $p < 0.0001$) compared to controls (0.21 ± 0.02 pg/mL, Fig. 6D). Likewise, administration of *G. vaginalis*- (0.34 ± 0.02 pg/mL, $p < 0.0001$) and *M. mulieris*-derived bEVs (0.19 ± 0.03 pg/mL, $p = 0.028$) increased TNF α production compared to PBS alone (0.08 ± 0.02 pg/mL, Fig. 6E). Exposure to *L. crispatus*- (8.36 ± 1.05 pg/mL, $p = 0.0006$), *G. vaginalis*- (7.91 ± 0.27 pg/mL, $p = 0.0071$), and *M. mulieris*-derived bEVs (23.44 ± 1.40 pg/mL, $p < 0.0001$) resulted in an increase in IP-10 concentration (Fig. 6F). MIP α concentration increase in response to *L. crispatus*- (5.18 ± 0.73 pg/mL, $p = 0.0012$), *G. vaginalis*- (7.15 ± 0.49 pg/mL, $p < 0.0001$), and *M. mulieris*-derived bEVs (10.00 ± 0.97 pg/mL, $p < 0.0001$, Fig. 6G). Lastly, *L. crispatus*- (1.31 ± 0.28 pg/mL, $p = 0.0069$), *G. vaginalis*- (1.25 ± 0.08 pg/mL, $p = 0.0300$), and *M. mulieris*-derived bEVs (2.43 ± 0.31 pg/mL, $p < 0.0001$) exposure resulted in an increase in MIP β compared to vehicle controls (0.35 ± 0.09 pg/mL, Fig. 6H).

In endometrial cells, *G. vaginalis*-derived bEVs (7.19 ± 0.14 pg/mL, $p < 0.0001$) resulted in an increase in IL-8 production compared to PBS alone (1.96 ± 0.17 pg/mL, Fig. 6I). No differences were seen in IL-6, IL-10, IP-10, and MIP α (Supplementary Fig. 7A–D).

In placental cells, *G. vaginalis*-derived bEVs (1.48 ± 0.13 pg/mL, $p = 0.0103$) resulted in an increase in TNF α production compared to PBS alone (Fig. 6J). No differences were observed in the production of IL-6, IL-8, IP-10, and MIP β (Supplementary Fig. 7E, F).

Discussion

The vaginal microbiome is significantly implicated in female reproductive health outcomes^{2,13,30}. Extensive clinical work establishes that dominance by

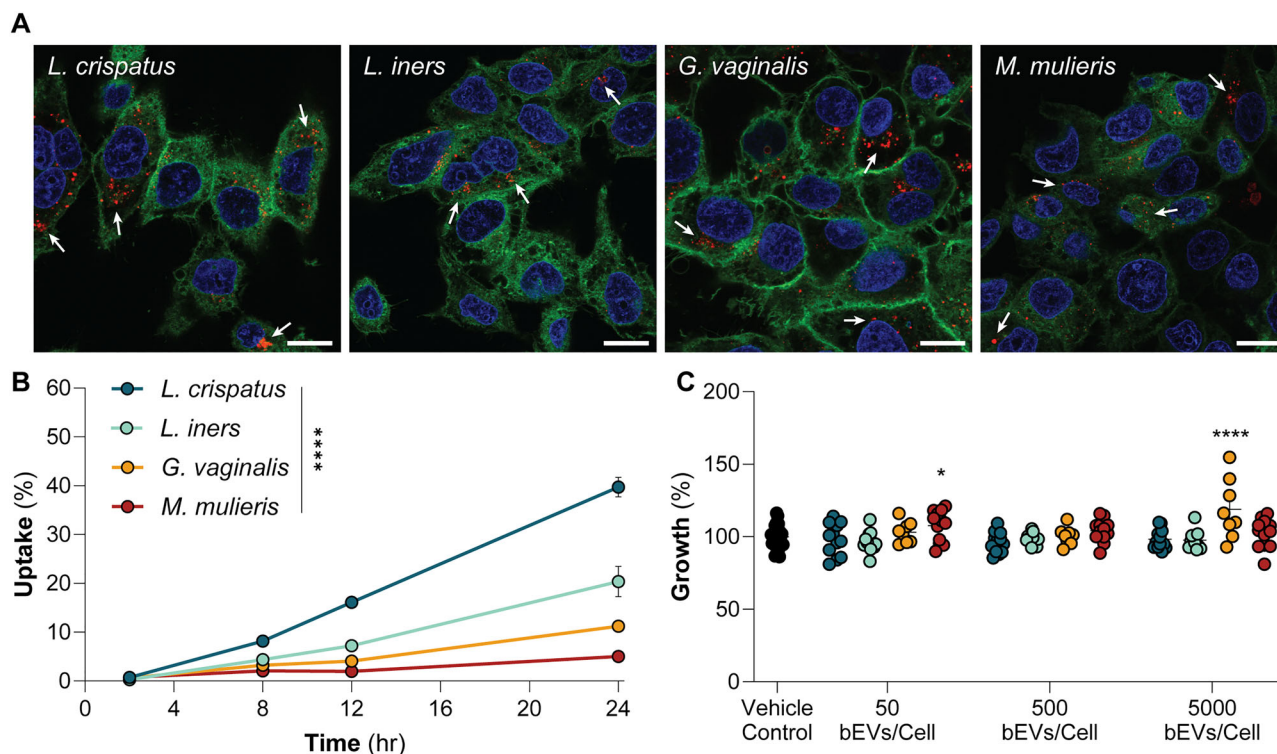


Fig. 5 | Placental cells internalize bEVs. **A** Confocal images reveal uptake of bEVs by placental cells in vitro. Scale bars denote 20 μm . **B** Placental cells internalize bEVs with *L. crispatus* > *L. iners* > *G. vaginalis* > *M. mulieris*. $n = 8-12$. **C** Increased cellular growth was observed after treatment with *M. mulieris*- and *G. vaginalis*-derived bEVs at 5000 bEVs/cell. $n = 8-16$. Statistics were performed using two-way

ANOVA. For viability experiments, Tukey post hoc multiple comparison tests were used to compare treatment groups to vehicle control. Outliers were removed in accordance with Grubb's outlier test. Data are shown as mean \pm SEM. (* $p \leq 0.05$, ** $p \leq 0.01$, *** $p \leq 0.001$, and **** $p \leq 0.0001$).

Lactobacillus spp. in the vaginal microbiome is associated with healthy outcomes, whereas a polymicrobial environment leads to increased risk for gynecologic, obstetric, and neonatal diseases³⁰. While the proximity of vaginal bacteria to the vaginal epithelium and cervix may facilitate direct microbial signaling, how the vaginal microbiome affects upper levels of the female reproductive tract is less well understood. One hypothesis surrounding microbial signaling to the upper female reproductive tract is the ascension of vaginal bacteria into the uterine environment, which could lead to functional changes to uterine and placental tissues. However, prior work from our group suggests that the CVM barrier would not permit the ascension of whole bacteria from the vagina into the uterus²². Instead, we hypothesize that communication between the vaginal microbiome and the female reproductive tract is, in part, modulated by bEVs derived from the vaginal microbiota.

Here, we isolated bEVs from human-derived, commercially available strains of *L. crispatus*, *L. iners*, *G. vaginalis*, and *M. mulieris*. We chose *L. crispatus* as representative of a healthy vaginal environment, *L. iners* as representative of a transitional environment, *G. vaginalis* as representative of dysbiosis, and *M. mulieris* as representative of advanced dysbiosis. Previous work investigated *L. crispatus*-, *G. vaginalis*-, and *M. mulieris*-derived bEVs, serving as a validation in our vaginal epithelial cell studies. Future studies should investigate bEVs derived from additional species and strains of relevant vaginal bacteria.

Consistent with previous work, we observe the diameter of bEVs to be 50-250 nm^{27,29,31,32}. We observed differences in bEV production rates, with *L. crispatus* and *L. iners* demonstrating higher productivity (bEVs/CFU) compared to dysbiotic species (*G. vaginalis* and *M. mulieris*). In the transition from a healthy to a dysbiotic vaginal environment, this loss of commensal or probiotic bEVs may reduce positive communication, increasing risk for adverse reproductive outcomes. Understanding differences in bEV activity within the vaginal microenvironment is critical to better

understanding and treating female reproductive diseases—both in terms of promoting healthy interactions and preventing dysbiotic interactions.

In order to deliver cargoes to female reproductive tissues, bEVs must be able to move through the protective CVM barrier. Previous work demonstrates a critical relationship between mucus barrier properties and risk for gynecologic and obstetric diseases^{17,18,20,22,33,34}. However, we hypothesized that, even with weakened barrier properties, dysbiotic mucus would prohibit direct interactions between bacterial cells and host cells. Indeed, we observed a significantly decreased mobility of whole microbes in comparison to bEVs of the same species, suggesting that it is unlikely that whole microbes can directly communicate with upper reproductive tissues. Of particular interest, even bEVs derived from *M. mulieris*, a motile bacterium, were significantly more mobile than parent cells, demonstrating that these bacteria are indeed hindered by the presence of CVM. We observe similarities in the MSD of *G. vaginalis* whole bacteria and *G. vaginalis*-derived bEVs, most notably in samples with $\text{pH} > 4.2$, which most likely contain higher levels of mucus degrading enzymes, as suggested by previous work^{20,22}. Although in this cohort we do not see significant differences in the mobility of whole bacteria and bEVs based on pH, this may be due to the low sample size ($n = 10$). Our data suggest that, as CVM barrier properties weaken in these dysbiotic samples, the mucus barrier may permit more “wiggling” of *G. vaginalis* parent cells. Regardless, the mobility of bEVs in CVM suggests the potential for these bacterial byproducts to reach upper reproductive tract tissues and facilitate signaling between vaginal microbiota and female reproductive tract tissues. Our results support emerging work in the EV and bEV fields demonstrating the ability of cell-derived nanoparticles to cross biological barriers, facilitating long-distance communication in the body³⁵⁻³⁹.

Vaginal epithelial cells form a tissue barrier to infections in the female reproductive tract. We observe that bEVs from all species were internalized by vaginal epithelial cells. *M. mulieris*-derived bEVs were more significantly internalized compared to *L. crispatus*-derived bEVs. As a dysbiotic species,

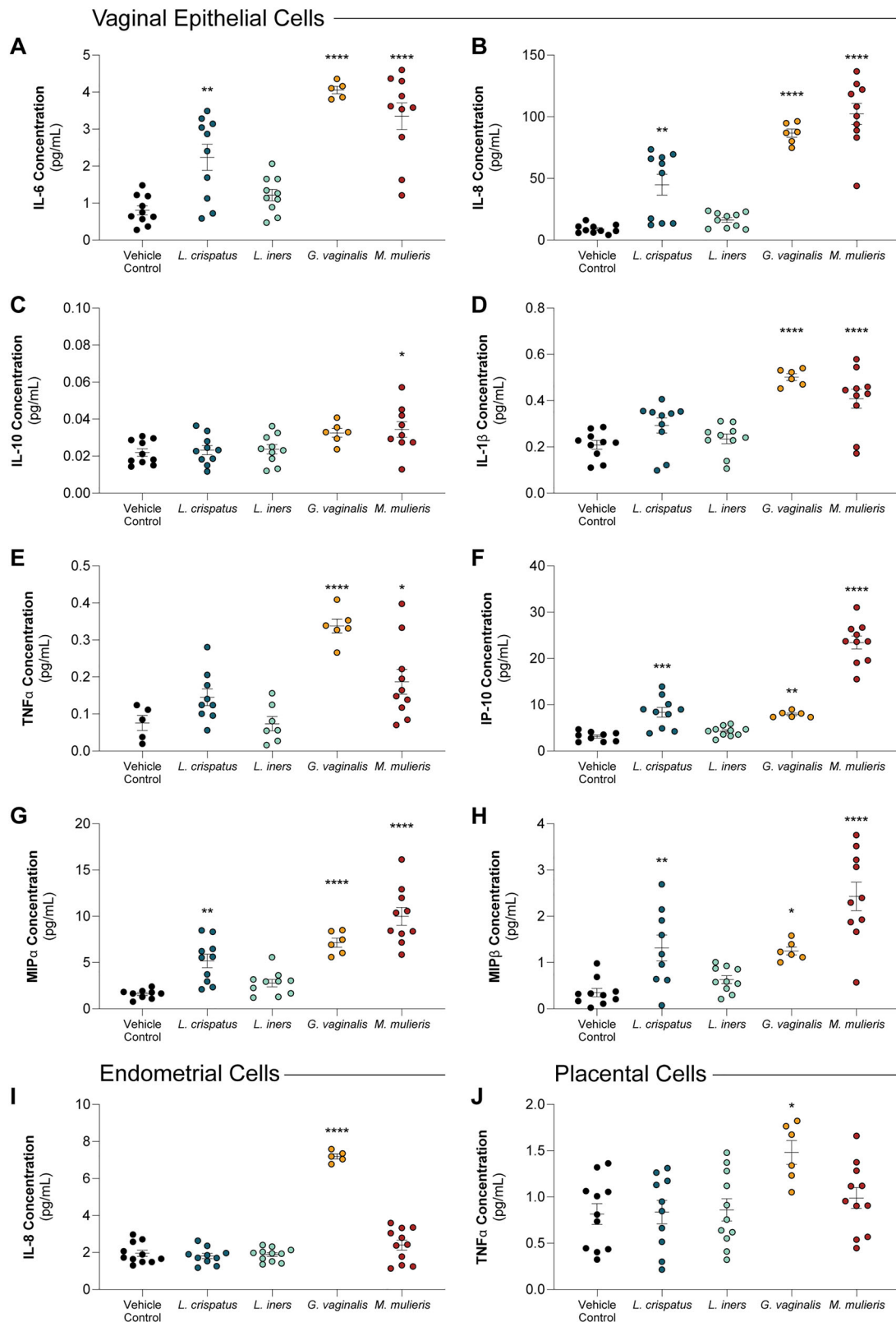


Fig. 6 | bEV administration modulates cytokine response in a species dependent manner. Vaginal epithelial cell production of **A** IL-6, **B** IL-8, **C** IL-10, **D** IL-1 β , **E** TNF α , **F** IP-10, **G** MIP α , and **H** MIP β was altered by exposure to bEVs. **I** *G. vaginalis*-derived bEVs increased IL-8 production in endometrial cells. **J** *G. vaginalis*-derived bEVs increased TNF α production in placental cells. bEVs were dosed

at 5000 bEVs/cell. Statistics were performed using one-way ANOVA with Tukey post hoc multiple comparison tests to compare treatment groups to the vehicle control for each cytokine. Outliers were removed in accordance with Grubb's outlier test. Data are shown as mean \pm SEM. (n = 6–11, * p \leq 0.05, ** p \leq 0.01, *** p \leq 0.001, and **** p \leq 0.0001).

the improved uptake of *M. mulieris*-derived bEVs may be potentially detrimental to reproductive tissues. Additionally, we observe changes to growth of cultured cells in response to bEV exposures, which may be attributed to specific bEV protein and metabolite cargoes. Future work should examine the clinical relevance of these findings using *in vivo* models.

Our data demonstrate that *G. vaginalis*- and *M. mulieris*-derived bEVs increase IL-6, IL-8, IL-10, IL-1 β , TNF α , IP-10, MIP α , and MIP β production in vaginal epithelium, indicative of a broad-inflammatory response. Previous work demonstrated the role of both *M. mulieris* whole bacteria and bEVs in modulation of cervicovaginal epithelial cells, activating immune response, and increasing production of metalloproteinase 9, which has been associated with risk of preterm birth⁴⁰. Additionally, the increased production of IL-6 by vaginal epithelial cells in response to *G. vaginalis*-derived and *M. mulieris*-derived bEVs is consistent with clinical reports of vaginal dysbiosis⁴¹. This supports recent work which explored the effects of *G. vaginalis*-derived bEVs *in vivo* using a mouse model⁴². In contrast, *L. crispatus* bEVs did not stimulate TNF α production, suggesting reduced potential for systemic inflammatory signaling, instead supporting localized immune priming and recruitment of protective immune cell populations within the vaginal environment. Previous literature demonstrates that *L. crispatus*-derived bEVs are capable of promoting wound healing and protective against HPV16 infection, supporting this hypothesis⁴³.

While some work has investigated bEV-mediated changes to lower female reproductive tract cells, no prior work has investigated vaginal bEV-mediated changes to endometrial cells. The endometrium plays a critical role in implantation, requiring a balance of pro- and anti-inflammatory signals⁴⁴. Previous work reported the presence of bacteria within endometrial samples, revealing an association between dysbiosis and decreased implantation rates^{45,46}. Our data demonstrate the uptake of bEVs by endometrial cells, as well as functional changes to inflammatory cytokine production. In particular, *G. vaginalis*-derived bEVs significantly increased the production of IL-8 in endometrial cells⁴⁷. These findings suggest that bEVs may, in part, mediate endometrial function.

Beyond vaginal epithelial and endometrial cells, microbial interactions with the placenta may impact preterm birth, as well as fetal programming^{35,48–51}. Even in full-term infants, maternal vaginal dysbiosis is associated increased risk for respiratory distress, low birthweight, neonatal sepsis, and admission to the neonatal intensive care unit⁸. bEVs have been shown to directly degrade placental barrier properties, demonstrating their ability to modulate tissue function³⁵. We report *in vitro* placental uptake of bEVs from all four species over the course of 24 h. Notably, *L. crispatus*-derived bEVs were most significantly internalized, suggesting the need for further understanding surrounding the lipid and protein composition that dictates *in vivo* interactions. Functionally, in a dysbiotic environment, the loss of probiotic-derived bEVs may exacerbate pro-inflammatory responses and negatively affect reproductive tissue function. Understanding microbe-host signaling in the placenta is critical to developing strategies that promote a healthy environment and healthy long-term development in offspring. Our observed increase in TNF- α production after exposure to *G. vaginalis*-derived bEVs may have implications in cell stress and death, which has been linked to preterm birth and other placental diseases⁵². Recent evidence of bEVs both in human placentas and infant meconium make bEV-placenta interactions a key area of interest^{36,37}.

In summary, our work is the first to examine the mobility of whole bacteria and bEVs in CVM and is the first to explore the interactions between vaginal microbe-derived bEVs and upper female reproductive tract cells. Our data suggests a novel role for bEVs in mediating microbe-host signaling relevant to gynecologic and obstetric diseases. While whole bacteria are unable to penetrate vaginal mucus, vaginal bacteria-derived bEVs can diffuse more freely to facilitate microbe-host communication in upper levels of the female reproductive tract. We also demonstrate that three different female reproductive tract cell lines can internalize bEVs from four vaginal microbe species. Beyond uptake, we report that bEVs mediate inflammatory response in reproductive cells, with relevance to bacterial vaginosis, endometriosis, preterm birth, and placental programming.

Future work should evaluate bEV-mediated microbe-host interactions using more complex models of the female reproductive tract, understand species- and strain-level differences in terms of bEV composition (especially using other dysbiosis-associated bacteria, such as *Prevotella bivia*), and leverage findings to develop next generation therapies for gynecologic and obstetric indications.

Methods

Materials

Human-derived strains of *Lactobacillus crispatus* (Brygoo and Aladame, 33820), *Lactobacillus iners* (BAA-3226), *Gardnerella vaginalis* (Gardner and Dukes, 14018), and *Mobiluncus mulieris* (43064), as well as VK2/E6E7 (CRL-2616), and Kaighn's Modification of Ham's F-12 media, were sourced from the American Type Culture Collection (ATCC, Manassas, VA). BeWo-b30 (CCL-98) cells were received as a generous gift Dr. John Fisher at the University of Maryland, College Park, and were originally sourced from ATCC (Manassas, VA). New York City III (NYCIII) media components (HEPES, proteose peptone, sodium chloride, dextrose, and yeast extract), PKH26 red fluorescent cell linker mini kit, bovine serum albumin (BSA), Gram staining materials (crystal violet, safranin, decolorizer, and iodine), calcium chloride, poly-L-lysine, Paraformaldehyde, and the Ishikawa cell line (99040201) were obtained from MilliporeSigma (Burlington, MA). Gibco™ horse serum, biconchonic acid assays (BCA), Amicon™ Ultra-15 Centrifugal Filter Units (10 kDa MWCO), Greiner Bio-One CELLSTAR μ Clear™ 96-well, Cell Culture-Treated, Flat-bottom Microplates, heat-inactivated fetal bovine serum (FBS), CellMask Deep Red, 4', 6-diamidino-2-phenylindole (DAPI), keratinocyte-serum free medium, epidermal growth factor, pituitary extract, L-glutamine, minimal essential medium (MEM), and non-essential amino acids (NEAA) were ordered from ThermoFisher Scientific (Waltham, MA). V-Plex Proinflammatory Panel 1 (human) kits and Chemokine Panel 1 Gen. B kits were purchased from MesoScale Discovery (Rockville, MD). SoftDisc menstrual discs (formerly SoftCup) were obtained from Amazon (National Landing, VA). Wiretrol® disposable micropipettes were obtained from Drummond Scientific Co. (Broomall, PA). Penicillin/Streptomycin was sourced from Corning (Corning, NY). μ -Slide 18 well glass bottom imaging wells were purchased from Ibidi (Fitchburg, Wisconsin). Cell Counting Kit-8 was purchased from APEXBio (Houston, TX). Formvar/Carbon 200 Mesh grids were sourced from Electron Microscopy Sciences (Hatfield, PA). 32 mL Open-Top Thickwall Polycarbonate Tubes (25 \times 89 mm), 38.5 mL Open-Top Thinwall Ultra-Clear Tubes (25 \times 89 mm), and 5 mL Open-Top Thinwall Polypropylene Tubes (13 \times 51 mm) were sourced from Beckman Coulter (Indianapolis, IN). Uranyl acetate was provided by the Laboratory for Biological Ultrastructure at the University of Maryland.

Bacteria culture

L. crispatus, *L. iners*, *G. vaginalis* and *M. mulieris* were cultured in particle-depleted NYCIII media. NYCIII media (0.4% w/v HEPES, 1.5% w/v proteose peptone, 0.5% w/v sodium chloride, 0.5% w/v dextrose, 2.6% w/v yeast extract) was supplemented with 10% v/v horse serum and prepared according to ATCC instructions. Particle-depleted media was prepared by ultracentrifugation using Thickwall ultracentrifuge tubes and a SW32Ti rotor (Beckman Coulter) at 100,000 \times g for 12–16 h followed by 0.2 μ m sterile filtration. All cultures were grown in anaerobic conditions (37 °C with 5% H₂, 10% CO₂, 85% N₂). Briefly, frozen stocks were plated on 1.5% w/v agar media using the four-quadrant streak method (Day 0), then transferred to 5 mL liquid cultures using an inoculating loop (Day 3). Five mL cultures were normalized via optical density at 600 nm (OD600) prior to transfer to 50 mL cultures (Day 6). To measure OD600, 100 μ L culture aliquots were taken from each culture and added to individual wells of a 96-well plate. Absorbance was read at 600 nm using a TECAN Spark® plate reader. Samples were diluted as needed to ensure an OD600 of <1. Optical densities were normalized and used to seed 50 mL cultures. Three days after seeding (Day 9), 10 μ L of culture was plated on NYCIII agar plates at 10⁻³ to 10⁻⁸ dilutions to determine the number of colony forming units (CFUs) present

in the sample. Plates were grown under anaerobic conditions for 2 days. Plates with 20–200 CFUs were considered within countable range.

bEV isolation

bEVs were isolated from conditioned media three days after seeding 50 mL cultures (Day 9), as previously described with modifications^{53–55}. Briefly, cultures were centrifuged at 4000 \times g for 20 min to remove whole bacteria. The resulting supernatant was then sequentially filtered through 0.45 and 0.2 μ m syringe filters. Filtered supernatant was ultracentrifuged using Thinwall ultracentrifuge tubes and a SW32Ti rotor (Beckman Coulter) at 16,000 \times g for 40 min to remove cell debris and aggregates. Supernatant was transferred to a new ultracentrifuge tube and centrifuged at 129,000 \times g for 1.5 h to isolate bEVs. The bEV pellet was resuspended in PBS and centrifuged at 129,000 \times g for 1.5 h to wash. Supernatant was discarded and the pellet was resuspended in the ~1 mL of PBS. Samples were characterized immediately following isolation.

bEV characterization

The size, ζ -potential, and concentration of each bEV sample were measured using nanoparticle tracking analysis (NTA, ZetaView, Particle Metrix, Meerbusch) ($n = 6$ for each species). bEV samples were diluted 1:1000. 11 positions were run to fully characterize the sample. Parameters were set to a minimum brightness of 65, a sensitivity of 85, a frame rate of 30, and a trace length of 15. The concentration of bEVs was normalized to the initial volume of conditioned media to account for differences in the volume of PBS used for resuspension. Concentrations are reported as particles per volume of conditioned media. Samples were normalized to CFUs by dividing the particles per volume of conditioned media by CFUs per volume of conditioned media. Protein content was measured via BCA and normalized to protein per 10^8 bEVs. Transmission electron microscopy (TEM) was completed at the University of Maryland Laboratory for Biological Ultrastructure. Samples were prepared at room temperature by depositing isolated bEVs on formvar/carbon 200 mesh grids. Samples were stained using 1% uranyl acetate. Images were taken using a HT7700 transmission electron microscope (Hitachi, Japan).

Labeling bacteria and bEVs

Whole bacteria were labeled using PKH26 Red Fluorescent Cell Linker Mini Kit, according to manufacturer's instructions, with modifications as previously described⁵⁶. Briefly, cultures were resuspended to an OD600 of 1.3. Samples were pelleted at 4,000 \times g for 20 min, and then resuspended in 2 mL of Diluent C. 4 μ g of PKH26 dye was added to the mixture and then incubated for 8 min at room temperature with gentle shaking. The reaction was quenched with 2 mL of FBS. Bacteria were pelleted at 4,000 \times g for 20 min and washed with PBS two times before the pellet was resuspended in 100 μ L PBS. Labeled bacteria were stored at 4 °C for up to 1 month.

bEVs were labeled, as previously described^{55,57}. Equal volumes of bEVs and PKH26 reagent were mixed at a ratio of 1×10^{10} bEVs per 0.8 μ g dye. The mixture was incubated for 5 min at room temperature with mixing by gentle pipetting. The reaction was quenched with an equal volume of BSA at a ratio of 1 mg per 1×10^{10} bEVs. Samples were immediately placed on top of a 2 mL 20% sucrose cushion and pelleted at 100,000 \times g for 2 h in Thinwall ultracentrifuge tubes and a SW55Ti rotor (Beckman Coulter). Pellets were resuspended in 5 mL of PBS and washed in a 15 mL 10 kDa MCWO filter. Samples were analyzed via NTA to determine final concentration⁵⁵. Labeled bEVs were stored at 4 °C for up to one week until use.

Cervicovaginal mucus collection

Human cervicovaginal mucus (CVM) was collected in accordance with protocol #2043110-3, as approved by the University of Maryland Institutional Review Board. Participants were determined to be in the luteal phase based on reported dates of menstruation and urine ovulation tests. Participants self-collected CVM using SoftDisc menstrual devices, as

previously described^{22,58}. Briefly, participants inserted the SoftDisc into the vagina for up to 1 min, and then removed the disc in a twisting motion to collect CVM. The SoftDisc was then placed into a 50 mL conical and spun at 300 \times g for 5 min to collect CVM. Samples were characterized via wet mount, and pH (Supp. Table 1). For wet mounts, <10 μ L of CVM was placed on a slide and smoothed using a wiretrol. 10 μ L normal saline was pipetted onto the sample to seal a coverslip. Slides were imaged on a ZEISS Axiovert 5 equipped with a 100x oil objective. The pH of each mucus sample was measured using a micro pH probe (MI-4146b, MicroElectrodes, Inc).

Multiple-particle tracking

Multiple-particle tracking (MPT) was conducted to assess the mobility of whole bacteria and bEVs in human CVM, as previously described^{22,55}. Three-dimensional wells were constructed using a 6 mm diameter hole punch through two layers of electrical tape adhered to a glass slide. 20 μ L of fresh CVM was added to the well along with 1.5 μ L of fluorescently labeled bacteria or bEVs. Particle mobility was recorded for 10–15 s at room temperature on a ZEISS Axiovert 5 equipped with a 100x oil objective. An Axiocam 305 Color camera was used to record videos at a frame rate of 14.78 frame/s. For each CVM sample, a minimum of 5 videos were taken for each particle type. The mean squared displacement (MSD) for each individual particle was calculated using image processing software in MATLAB, as previously described ($n = 10$ CVM samples)^{22,55}.

Cell culture

VK2/E6E7 vaginal epithelial cells were cultured in keratinocyte-serum free medium supplemented with 0.1 ng/mL human recombinant EGF, 0.05 mg/mL bovine pituitary extract, and additional 44.1 mg/L calcium chloride, according to manufacturer's instructions. Experiments utilized passages 5–18. Ishikawa endometrial cells were cultured in MEM media supplemented with 2 mM L-glutamine, 1% v/v NEAA, and 5% v/v FBS, according to manufacturer's instructions. Experiments utilized passages 6–10. For VK2/E6E7 and Ishikawa cell lines, media was exchanged every 48–72 h until confluent. BeWo-b30 placental cells were cultured in F-12K supplemented with 10% v/v FBS and 1% v/v penicillin/streptomycin. Experiments utilized passages 24–33. Media was exchanged every 24–48 h until confluency. All cell lines were maintained at 37 °C, 5% CO₂. Cells were passaged at 85–95% confluency.

bEV uptake

Cells were seeded at 0.04 $\times 10^6$ cells per well in a black walled 96-well plate and allowed to adhere overnight. Media was exchanged immediately before dosing wells with 2500 labeled bEVs/cell. Uptake was measured 2, 8, 12, and 24 h after dosing ($n = 8–12$ wells/timepoint). Cells were washed with PBS three times before incubation with 1% Triton for 1 h, as previously described⁵⁹. Fluorescent readings were taken at 530:567 nm to determine internalized bEV concentrations. Standard curves were created using known concentrations of bEVs in 1% Triton. Values below the limit of detection were assigned a value of zero.

For confocal imaging, μ -Slide glass bottom 18-well plates were treated with poly-L-lysine for 20 min and dried overnight. Cells were seeded at 0.04 $\times 10^6$ cells/well and allowed to adhere overnight. Media was exchanged immediately prior to dosing with labeled bEVs. Labeled bEVs (labeled via PKH26, see above) were added to each well at a concentration of 2500 bEVs/cell. After 24 h, media was removed, and cells were washed with PBS two times to remove any extracellular bEVs. Cells were then labeled with Cell-Mask Deep Red membrane stain for 5–10 min, according to manufacturer's instructions. Cells were fixed via incubation with 2% w/v formaldehyde at 37 °C for 5 min and washed with PBS three times. Cells were incubated in 300 nM DAPI for 5 min and washed with PBS according to manufacturer's instructions. Cells were imaged using a LSM 980 Laser Scanning Confocal microscope (Zeiss, Oberkochen, Germany; $n = 3$ images per well, 3 wells per condition).

Cell viability

Cells were seeded at 0.04×10^6 cells per well in a 96-well plate and allowed to adhere overnight. Media was exchanged immediately before dosing wells with 50, 500, or 5000 bEVs per cell. After 24 h, Cell Counting Kit-8 (CCK-8) was used according to manufacturer's instructions. Briefly, 10 μ L of assay reagent was added to each well. Samples were incubated at 37 °C for 1 h. Viability was determined by measuring the OD450 and normalizing to background (OD600). Cell viability was normalized to vehicle control (PBS) (n = 8–16 per treatment group).

Multiplex assays

Cells were seeded at 0.24×10^6 in a 24-well plate and allowed to adhere overnight. Media was exchanged immediately before dosing wells with 5000 bEVs per cell. Samples were incubated for 24 h, after which supernatants were collected and stored at -80 °C until use. IL-1 β , IL-6, IL-8, IL-10, TNF- α , MIP-1 β , IP-10, and MIP-1 α cytokines were measured using custom V-PLEX plates, according to the manufacturer's instructions. Wells were first washed three times according to manufacturer's instructions. Samples were diluted as needed in the supplied sample buffer, and 50 μ L of diluted sample was added to appropriate wells. Plates were incubated at RT for 2 h while shaking at 700 rpm. After washing three times, 25 μ L of detection antibody solution was added to each well, and the plate was incubated at RT while shaking for 2 h at 700 rpm. The plate was washed three times and 150 μ L of read buffer was added to each well by reverse pipetting. The plate was immediately read using the MSD Meso Quickplex SQ 120MM Imager. Cytokine concentration (n = 6–11 per condition) was calculated based on a standard curve run on each plate using Discovery Workbench software from MSD.

Statistical analysis

GraphPad Prism was used for statistical analysis. For bEV characterizations and multiplex immunoassays, one-way analysis of variance (ANOVA) testing was used. Viability and cellular uptake studies were analyzed via two-way ANOVA. Statistical significance was defined as $p < 0.05$. For bEV characteristics, multiplexed immunoassays, and viability, Tukey post hoc multiple comparisons were used to determine statistical significance between groups. For uptake studies, replicates were assigned as zero if fluorescent values were below the standard curve. For multiple-particle tracking analysis, two-tailed Mann-Whitney non-parametric tests were performed to compare whole bacteria and bEV mobility in each individual participant, as previously described⁶⁰. Statistics between the geometric mean of MSDs were determined using Wilcoxon matched-pairs signed rank tests for each bEV-whole bacterial pair. For characterization, uptake, and viability experiments, outliers were removed according to Grubb's outlier test with significance at $p < 0.05$. Data are presented as mean \pm standard error of the mean (SEM).

Data availability

All data generated or analyzed during this study are included in this published article and its supplementary information file. Data may be found at: <https://doi.org/10.5061/dryad.cvdncjth8>.

Received: 22 April 2025; Accepted: 10 November 2025;

Published online: 09 January 2026

References

- Human Microbiome Project, C Structure, function and diversity of the healthy human microbiome. *Nature* **486**, 207–214 (2012).
- Ravel, J. et al. Vaginal microbiome of reproductive-age women. *Proc. Natl. Acad. Sci. USA* **108**, 4680–4687 (2011).
- Mousavi, E. et al. Antiviral effects of *Lactobacillus crispatus* against HSV-2 in mammalian cell lines. *J. Chin. Med. Assoc.* **81**, 262–267 (2018).
- Parolin, C. et al. Isolation of vaginal *Lactobacilli* and characterization of anti-*Candida* activity. *PLoS One* **10**, e0131220 (2015).
- Scillato, M. et al. Antimicrobial properties of *Lactobacillus* cell-free supernatants against multidrug-resistant urogenital pathogens. *MicrobiologyOpen* **10**, e1173 (2021).
- Peebles, K., Velloza, J., Balkus, J. E., McClelland, R. S. & Barnabas, R. V. High global burden and costs of bacterial vaginosis: a systematic review and meta-analysis. *Sex. Transmitted Dis.* **46**, 304–311 (2019).
- Spiegel, C. A. Bacterial vaginosis. *Clin. Microbiol. Rev.* **4**, 485–502 (1991).
- Dingens, A. S., Fairfortune, T. S., Reed, S. & Mitchell, C. Bacterial vaginosis and adverse outcomes among full-term infants: a cohort study. *BMC Pregnancy Childbirth* **16**, 1–8 (2016).
- Nelson, D. B., Hanlon, A. L., Wu, G., Liu, C. & Fredricks, D. N. First trimester levels of BV-associated bacteria and risk of miscarriage among women early in pregnancy. *Matern. Child Health J.* **19**, 2682–2687 (2015).
- Eschenbach, D. A. Bacterial vaginosis and anaerobes in obstetric-gynecologic infection. *Clin. Infect. Dis.* **16**, S282–S287 (1993).
- Atashili, J., Poole, C., Ndumbe, P. M., Adimora, A. A. & Smith, J. S. Bacterial vaginosis and HIV acquisition: a meta-analysis of published studies. *Aids* **22**, 1493–1501 (2008).
- Anton, L. et al. *Gardnerella vaginalis* alters cervicovaginal epithelial cell function through microbe-specific immune responses. *Microbiome*. **10**, 119 (2022).
- Elovitz, M. A. et al. Cervicovaginal microbiota and local immune response modulate the risk of spontaneous preterm delivery. *Nat. Commun.* **10**, 1305 (2019).
- Lewis, W. G., Robinson, L. S., Gilbert, N. M., Perry, J. C. & Lewis, A. L. Degradation, foraging, and depletion of mucus sialoglycans by the vagina-adapted *Actinobacterium Gardnerella vaginalis**. *J. Biol. Chem.* **288**, 12067–12079 (2013).
- Cauci, S., Culhane, J. F., Di Santolo, M. & McCollum, K. Among pregnant women with bacterial vaginosis, the hydrolytic enzymes sialidase and proliadase are positively associated with interleukin-1 β . *Am. J. Obstet. Gynecol.* **198**, 132.e131–132.e137 (2008).
- Chen, C. et al. The microbiota continuum along the female reproductive tract and its relation to uterine-related diseases. *Nat. Commun.* **8**, 875 (2017).
- Tsiligianni, T., Karagiannidis, A., Brikas, P. & Saratsis, P. Chemical properties of bovine cervical mucus during normal estrus and estrus induced by progesterone and/or PGF2 α . *Theriogenology* **56**, 41–50 (2001).
- Adnane, M., Meade, K. G. & O'Farrelly, C. Cervico-vaginal mucus (CVM) – an accessible source of immunologically informative biomolecules. *Vet. Res. Commun.* **42**, 255–263 (2018).
- Cone, R. A. Barrier properties of mucus. *Adv. Drug Deliv. Rev.* **61**, 75–85 (2009).
- Hoang, T. et al. The cervicovaginal mucus barrier to HIV-1 is diminished in bacterial vaginosis. *PLoS Pathog.* **16**, e1008236 (2020).
- Robinson, L. S., Schwebke, J., Lewis, W. G. & Lewis, A. L. Identification and characterization of NanH2 and NanH3, enzymes responsible for sialidase activity in the vaginal bacterium *Gardnerella vaginalis*. *J. Biol. Chem.* **294**, 5230–5245 (2019).
- Zierden, H. C. et al. Cervicovaginal mucus barrier properties during pregnancy are impacted by the vaginal microbiome. *Front. Cell. Infect. Microbiol.* **13**, <https://doi.org/10.3389/fcimb.2023.1015625> (2023).
- Hosseini-Giv, N. et al. Bacterial extracellular vesicles and their novel therapeutic applications in health and cancer. *Front. Cell. Infect. Microbiol.* **12**, <https://doi.org/10.3389/fcimb.2022.962216> (2022).
- Xie, J., Li, Q., Haesebrouck, F., Van Hoecke, L. & Vandembroucke, R. E. The tremendous biomedical potential of bacterial extracellular vesicles. *Trends Biotechnol.* **40**, 1173–1194 (2022).
- Schertzer, J. W. & Whiteley, M. A bilayer-couple model of bacterial outer membrane vesicle biogenesis. *mBio* **3**, <https://doi.org/10.1128/mBio.00297-11> (2012).

26. Kirian, R. D., Steinman, D., Jewell, C. M. & Zierden, H. C. Extracellular vesicles as carriers of mRNA: Opportunities and challenges in diagnosis and treatment. *Theranostics* **14**, 2265–2289 (2024).
27. Joseph, A. et al. Extracellular vesicles from vaginal *Gardnerella vaginalis* and *Mobiluncus mulieris* contain distinct proteomic cargo and induce inflammatory pathways. *npj Biofilms Microbiomes* **10**, 28 (2024).
28. Moore, K. A., Petersen, A. P. & Zierden, H. C. Microorganism-derived extracellular vesicles: emerging contributors to female reproductive health. *Nanoscale* **16**, 8216–8235 (2024).
29. Nahui Palomino, R. A. et al. Extracellular vesicles from symbiotic vaginal lactobacilli inhibit HIV-1 infection of human tissues. *Nat. Commun.* **10**, 5656 (2019).
30. Ma, B., Fomey, L. J. & Ravel, J. Vaginal microbiome: rethinking health and disease. *Annu. Rev. Microbiol.* **66**, 371–389 (2012).
31. Shishpal, P., Kasarpalkar, N., Singh, D. & Bhor, V. M. Characterization of *Gardnerella vaginalis* membrane vesicles reveals a role in inducing cytotoxicity in vaginal epithelial cells. *Anaerobe* **61**, 102090 (2020).
32. Fakharian, F., Sadeghi, A., Pouresmaeili, F., Soleimani, N. & Yadegar, A. Anti-inflammatory effects of extracellular vesicles and cell-free supernatant derived from *Lactobacillus crispatus* strain RIGLD-1 on *Helicobacter pylori*-induced inflammatory response in gastric epithelial cells in vitro. *Folia Microbiol.* **69**, 927–939 (2024).
33. Zierden, H. C. et al. Avoiding a sticky situation: bypassing the mucus barrier for improved local drug delivery. *Trends Mol. Med.* **27**, 436–450 (2021).
34. Critchfield, A. S. et al. Cervical mucus properties stratify risk for preterm birth. *PLoS One* **8**, e69528 (2013).
35. Surve, M. V. et al. Membrane vesicles of group B *Streptococcus* disrupt fetomaternal barrier leading to preterm birth. *PLoS Pathog.* **12**, e1005816 (2016).
36. Turunen, J. et al. Bacterial extracellular vesicles in the microbiome of first-pass meconium in newborn infants. *Pediatr. Res.* **93**, 887–896 (2023).
37. Menon, R. et al. Amplification of microbial DNA from bacterial extracellular vesicles from human placenta. *Front. Microbiol.* **14**, <https://doi.org/10.3389/fmicb.2023.1213234> (2023).
38. Shah, N. et al. Extracellular vesicle-mediated long-range communication in stressed retinal pigment epithelial cell monolayers. *Biochim. Biophys. Acta (BBA) Mol. Basis Dis.* **1864**, 2610–2622 (2018).
39. Díaz-Garrido, N., Badia, J. & Baldomà, L. Microbiota-derived extracellular vesicles in interkingdom communication in the gut. *J. Extracell. Vesicles* **10**, e12161 (2021).
40. Hasegawa, Y. et al. *Mobiluncus mulieris* alters the transcriptomic profile of cervicovaginal epithelial cells, shedding light on molecular drivers of adverse reproductive outcomes. *npj Biofilms Microbiomes* **11**, 154 (2025).
41. Taylor, B. D. et al. Inflammation biomarkers in vaginal fluid and preterm delivery. *Hum. Reprod.* **28**, 942–952 (2013).
42. Shin, Y. J., Ma, X., Baek, J. S. & Kim, D. H. The Vaginally Exposed Extracellular Vesicle of *Gardnerella vaginalis* Induces RANK/RANKL-Involved Systemic Inflammation in Mice. *Microorganisms* **13**, <https://doi.org/10.3390/microorganisms13040955> (2025).
43. Peng, K. et al. *Lactobacillus crispatus*-derived nCEV vesicles promote cutaneous wound healing and inhibit HPV16 infection. *mSystems* **10**, e00683–00625 (2025).
44. Maybin, J. A., Critchley, H. O. D. & Jabbour, H. N. Inflammatory pathways in endometrial disorders. *Mol. Cell. Endocrinol.* **335**, 42–51 (2011).
45. Lozano, F. M. et al. Characterization of the endometrial microbiome in patients with recurrent implantation failure. *Microorganisms* **11**, 741 (2023).
46. Ichihama, T. et al. Analysis of vaginal and endometrial microbiota communities in infertile women with a history of repeated implantation failure. *Reprod. Med. Biol.* **20**, 334–344 (2021).
47. Arici, A. Local cytokines in endometrial tissue: the role of interleukin-8 in the pathogenesis of endometriosis. *Ann. N. Y. Acad. Sci.* **955**, 101–109 (2002).
48. Jasarevic, E. et al. The composition of human vaginal microbiota transferred at birth affects offspring health in a mouse model. *Nat. Commun.* **12**, 6289 (2021).
49. Jasarevic, E. et al. The maternal vaginal microbiome partially mediates the effects of prenatal stress on offspring gut and hypothalamus. *Nat. Neurosci.* **21**, 1061–1071 (2018).
50. Zierden, H. C. et al. Extracellular vesicles are dynamic regulators of maternal glucose homeostasis during pregnancy. *Sci. Rep.* **13**, 4568 (2023).
51. Rautava, S., Collado, M. C., Salminen, S. & Isolauri, E. Probiotics modulate host-microbe interaction in the placenta and fetal gut: a randomized, double-blind, placebo-controlled trial. *Neonatology* **102**, 178–184 (2012).
52. Yeganegi, M. et al. Effect of *Lactobacillus rhamnosus* GR-1 supernatant and fetal sex on lipopolysaccharide-induced cytokine and prostaglandin-regulating enzymes in human placental trophoblast cells: implications for treatment of bacterial vaginosis and prevention of preterm labor. *Am. J. Obstet. Gynecol.* **200**, 532.e531–532.e538 (2009).
53. Dean, S. N. et al. *Lactobacillus acidophilus* membrane vesicles as a vehicle of bacteriocin delivery. *Front. Microbiol.* **11**, <https://doi.org/10.3389/fmicb.2020.00710> (2020).
54. Caruana, J. C., Dean, S. N. & Walper, S. A. Isolation and characterization of membrane vesicles from *Lactobacillus* species. *Bio-Protoc.* **11**, e4145–e4145 (2021).
55. Steinman, D., Kirian, R. D. & Zierden, H. C. in *Bacterial Extracellular Vesicles: Methods and Protocols* (eds Steven Jay & Nicholas Pirolli) 137–152 (Springer US, 2024).
56. Batoni, G. et al. *Lactobacillus* probiotic strains differ in their ability to adhere to human lung epithelial cells and to prevent adhesion of clinical isolates of *Pseudomonas aeruginosa* from cystic fibrosis lung. *Microorganisms* **11**, 1707 (2023).
57. Kwak, G. et al. Extracellular vesicles enhance pulmonary transduction of stably associated adeno-associated virus following intratracheal administration. *J. Extracell. Vesicles* **12**, 12324 (2023).
58. Boskey, E. R., Moench, T. R., Hees, P. S. & Cone, R. A. A self-sampling method to obtain large volumes of undiluted cervicovaginal secretions. *Sex. Transmitted Dis.* **30**, 107–109 (2003).
59. Jiang, Z. et al. Placental cell translocation of folate-conjugated pullulan acetate non-spherical nanoparticles. *Colloids Surf. B: Biointerfaces* **216**, 112553 (2022).
60. Kaler, L. et al. Influenza A virus diffusion through mucus gel networks. *Commun. Biol.* **5**, 249 (2022).

Acknowledgements

This work was funded by a Faculty-Student Research Award from the Graduate School, University of Maryland (HCZ), the Minta Martin Foundation (HCZ) We acknowledge the support of the University of Maryland, Baltimore, Institute for Clinical & Translational Research (ICTR) and the National Center for Advancing Translational Sciences (NCATS) Clinical Translational Science Award (CTSA), UM1TR004926, as well as the University of Maryland Strategic Partnership: MPowering the State (MPower) (DS, HCZ). DS was supported by the Microbiome Summer Support Fellowship through the Center of Excellence in Microbiome Sciences. APP was supported by the Clark Doctoral Fellows Program through the A. James Clark School of Engineering. Purchase of the Zeiss LSM 980 Airyscan 2 was supported by Award Number 1S10OD025223-01A1 from the National Institute of Health. Funders played no role in the study design, data collection, analysis and interpretation of data, or the writing of the manuscript. Finally, we would like to thank Dr. Senta Kapnick from Dr. Christopher Jewell's Laboratory and Dr. Chen-Yu Chen from Dr. William Bentley's Laboratory for their insight and use of equipment throughout this work.

Author contributions

D.S. and H.C.Z. conceptualized the study. D.S., A.P.P., Y.C., C.C., and P.T. performed and analyzed experiments. D.S. wrote the original draft. D.S., A.P.P., and H.C.Z. reviewed and edited the manuscript. All authors read and approved the final manuscript.

Competing interests

The authors declare no competing interests.

Additional information

Supplementary information The online version contains supplementary material available at <https://doi.org/10.1038/s41522-025-00866-9>.

Correspondence and requests for materials should be addressed to Hannah C. Zierden.

Reprints and permissions information is available at <http://www.nature.com/reprints>

Publisher's note Springer Nature remains neutral with regard to jurisdictional claims in published maps and institutional affiliations.

Open Access This article is licensed under a Creative Commons Attribution-NonCommercial-NoDerivatives 4.0 International License, which permits any non-commercial use, sharing, distribution and reproduction in any medium or format, as long as you give appropriate credit to the original author(s) and the source, provide a link to the Creative Commons licence, and indicate if you modified the licensed material. You do not have permission under this licence to share adapted material derived from this article or parts of it. The images or other third party material in this article are included in the article's Creative Commons licence, unless indicated otherwise in a credit line to the material. If material is not included in the article's Creative Commons licence and your intended use is not permitted by statutory regulation or exceeds the permitted use, you will need to obtain permission directly from the copyright holder. To view a copy of this licence, visit <http://creativecommons.org/licenses/by-nc-nd/4.0/>.

© The Author(s) 2025